HHS Public Access

Author manuscript

J Proteome Res. Author manuscript; available in PMC 2019 June 03.

Published in final edited form as:

J Proteome Res. 2015 September 04; 14(9): 4050–4058. doi:10.1021/acs.jproteome.5b00596.

Effects of Dietary Different Doses of Copper and High Fructose Feeding on Rat Fecal Metabolome

Xiaoli Wei[#†,¶], **Ming Song**[#⊥], **Xinmin Yin**[†,¶], **Dale A. Schuschke**[§], **Imhoi Koo**[†,¶], **Craig J. McClain**[*,⊥,‡,‖], and **Xiang Zhang**[*,†,¶,‡]

[†]Department of Chemistry, University of Louisville, Louisville, Kentucky 40292, United States

[‡]Department of Pharmacology and Toxicology, University of Louisville, Louisville, Kentucky 40292, United States

[§]Department of Physiology and Biophysics, University of Louisville, Louisville, Kentucky 40292, United States

[⊥]Department of Medicine, University of Louisville, Louisville, Kentucky 40292, United States

[¶]Center for Regulatory and Environmental Analytical Metabolomics, University of Louisville, Louisville, Kentucky 40292, United States

[‖]Robley Rex Louisville VAMC, Louisville, Kentucky 40292, United States

[#] These authors contributed equally to this work.

Abstract

The gut microbiota plays a critical role in the pathogenesis of nonalcoholic fatty liver disease (NAFLD). Increased fructose consumption and inadequate copper intake are two critical risk factors in the development of NAFLD. To gain insight into the role of gut microbiota, fecal metabolites, obtained from rats exposed to different dietary levels of copper with and without high fructose intake for 4 weeks, were analyzed by comprehensive two-dimensional gas chromatography time-of-flight mass spectrometry (GC × GC-TOF MS). In parallel, liver tissues were assessed by histology and triglyceride assay. Our data showed that high fructose feeding led to obvious hepatic steatosis in both marginal copper deficient rats and copper supplementation rats. Among the 38 metabolites detected with significant abundance alteration between groups, short chain fatty acids were markedly decreased with excessive fructose intake irrespective of copper levels. C15:0 and C17:0 long chain fatty acids, produced only by bacteria, were increased by either high copper level or high fructose intake. In addition, increased fecal urea and malic acid paralleled the increased hepatic fat accumulation. Collectively, GC × GC-TOF MS analysis of rat fecal samples revealed distinct fecal metabolome profiles associated with the dietary high fructose

[*]**Corresponding Authors** Phone: +01 502 852 2912. Fax: +01 502 852 2912. craig.mcclain@louisville.edu, Phone: +01 502 852 8878. Fax: +01 502 852 8149. xiang.zhang@louisville.edu.

The authors declare no competing financial interest.

ASSOCIATED CONTENT

Supporting Information

The Supporting Information is available free of charge on the ACS Publications website at DOI: 10.1021/acs.jproteome.5b00596. Cross-validation of the PLSDA model; IPA proof-of- knowledge characterization of metabolic networks in rat fecal metabolome (PDF)

and copper level, with some metabolites possibly serving as potential noninvasive biomarkers of fructose induced-NAFLD.

GRAPHICAL ABSTRACT

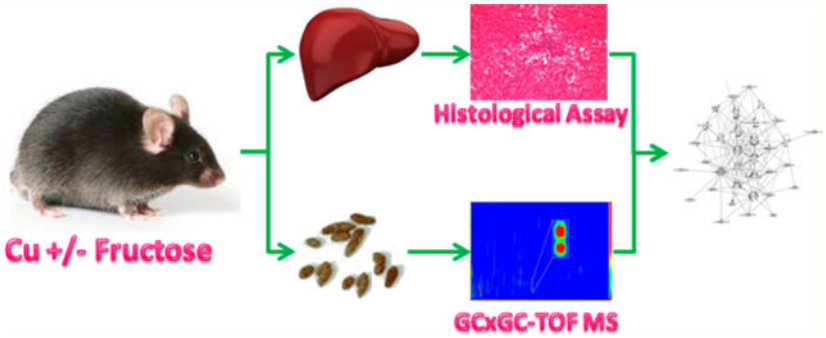

Keywords

GC × GC-TOF MS; metabolomics; nonalcoholic fatty liver disease; fructose; copper

1. INTRODUCTION

Nonalcoholic fatty liver disease (NAFLD) has emerged as the most common liver disease in the developed countries. As a spectrum of diseases, NAFLD ranges from simple steatosis to nonalcoholic steatohepatitis (NASH) to fibrosis and cirrhosis, and potentially to hepatocellular carcinoma. As of 2011, the prevalences of NAFLD and NASH were reported to be 46% and 12.2%, respectively, in the United States.[1] Moreover, NAFLD is strongly associated with obesity as well as insulin resistance and type II diabetes and is considered to be the hepatic manifestation of metabolic syndrome.[2,3] Among the patients with simple steatosis, 12–40% will progress to NASH after 8–13 years.[4]

Despite significant progress, the pathogenesis and development of NAFLD remain incompletely understood. The rapid rise in the prevalence of NAFLD suggests a possible role of environmental factors in the pathogenesis of this disease. Increased fructose consumption parallels the increased prevalence of obesity and the metabolic syndrome in the United States.[5,6] NAFLD patients have been shown to have excessive fructose consumption,[7] which most likely can be attributed to the increased use of high fructose corn syrup (HFCS). In addition, a growing body of evidence supports the causative role of fructose in the increased rates of obesity and metabolic phenotypes.[8–10] It is well-known that fructose is a highly lipogenic sugar due to its unique metabolic pathway, which bypasses the rate-limiting enzyme phosphofructokinase and leads to rapid hepatic *de novo* lipogenesis.[11] On the other hand, because of the limited absorption in the upper gastrointestinal tract, the unabsorbed fructose goes to the distal intestine, which may cause gut bacterial overgrowth, gut barrier dysfunction, and endotoxemia.[12,13] The results of gut bacterial overgrowth may lead not only to increased gut permeability, but also to a change of intestine luminal metabolites, both of which may contribute to the pathogenesis of NAFLD.

Inadequate copper intake represents another important nutritional issue in the United States. Extensive studies, including ours, have shown that dietary fructose–copper interactions impair copper status and exacerbate the phenotypes of the metabolic syndrome, in particular, hepatic fat accumulation.[14–16] Importantly, NAFLD patients have been shown to have lower copper availability. Moreover, a copper- deficient diet induces fatty liver in rodents.[17,18]

Taken together, increased fructose consumption and inadequate copper intake are two critical risk factors in the pathogenesis of NAFLD. However, their combinational role in the alteration of gut metabolites remains unknown. In the current study, we employed a metabolomics approach to study the effects of different dietary doses of copper combined with high fructose feeding on the homeostasis of intestine luminal metabolites to understand the pathogenesis of NAFLD. Male weanling Sprague–Dawley rats were exposed to three different levels of copper for a period of 4 weeks, with and without high fructose coexposure. Liver and fecal samples were collected at the end of the feeding period. The liver samples were used for histological study, while the metabolite extracts from rat feces were analyzed using comprehensive two-dimensional gas chromatography time-of-flight mass spectrometry (GC × GC- TOF MS) for metabolic profiling.

2. EXPERIMENTAL METHODS

2.1 Animals and Diets

Male weanling Sprague–Dawley rats (35–45 g) from the Harlan Laboratories (Indianapolis, IN) were fed (*ad lib*) a purified AIN-76 diet with a defined copper content in form of cupric carbonate. The rats received 1.6, 6.0, or 20 ppm of copper as marginal, adequate, or supplemental doses, respectively. The animals were housed in stainless steel cages in a temperature- and humidity-controlled room with a 12:12 h light–dark cycle. Animals had free access to either deionized water or deionized water containing 30% fructose (w/v) during the entire 4 week feeding period. Fructose enriched drinking water was changed twice each week. At the end of the feeding period, all animals were killed under anesthesia with pentobarbital (50 mg/kg I.P. injection) after overnight fasting. The colon fecal samples and liver tissues were collected from each rat. All fecal samples were immediately snap-frozen with liquid nitrogen. Portions of liver tissue were fixed with 10% formalin for subsequent sectioning, while other sections were snap-frozen with liquid nitrogen. All studies were approved by the University of Louisville Institutional Animal Care and Use Committee, which is certified by the American Association of Accreditation of Laboratory Animal Care.

2.2. Histological Analysis

Formalin-fixed, paraffin-embedded liver tissue sections were cut at 5 μm thickness. Sections were stained with hematoxylin and eosin (H&E).

2.3. Hepatic Triglyceride Assay

Liver tissues were homogenized in ice-cold phosphate buffered saline. Hepatic total lipids were extracted using solvent chloroform/methanol (2:1) according to the method described by Bligh and Dyer.[19] The lipids extracted in chloroform were first dried and then redissolved

in 2% Triton X-100 in water. Hepatic triglyceride content was determined by commercially available kits (Infinity, Thermo Electron, Melbourne, Australia).

2.4. Metabolite Sample Preparation

Rat colon fecal samples were prepared following the protocol described in detail in our previous work.[20] Briefly, each fecal sample was first weighed and homogenized on ice. Each homogenized fecal sample was added to ice cold 80% methanol with a ratio of 50 mg of feces in 1 mL of 80% methanol. The mixture was vortexed for 10 min, followed by centrifugation for 10 min at 15 000 rpm. Four-hundred microliters of the supernatant was aspirated into a glass vial and dried by SpeedVac overnight at 14 °C. The dried metabolite extracts were dissolved in 40 μL of the methoxyamine hydrochloride solution in pyridine (20 mg/mh) and vigorously vortex-mixed for 2 min. Methoxymation was carried out at 70 °C for 30 min. After the addition of 40 μL of N-(tert-butyldimethylsilyl)-N methyltrifluoroacetamide (MTBSTFA) mixed with 1% *tert*- butyldimethylchlorosilane (TBDMSCI), derivatization was carried out at 70 °C for 1 h.

To verify metabolite identification, commercially available authentic standards of metabolites detected with significant abundance alteration between sample groups were prepared in equal molarity and analyzed by GC × GC-TOF MS. The methoxymation and derivatization of the fecal samples and compound standards were carried out right before GC × GC- TOF MS analysis, respectively.

2.5. GC × GC-TOF MS Analysis

The LECO Pegasus 4D GC × GC-TOF MS instrument was equipped with an Agilent 6890 gas chromatograph and a Gerstel MPS2 autosampler (GERSTEL Inc., Linthicum, MD) featuring a LECO two-stage cryogenic modulator and secondary oven. The primary column was a 60 m × 0.25 mm ${}^1d_c$ × 0.25 μm ${}^1d_f$, DB-5 ms GC capillary column (phenyl arylene polymer virtually equivalent to a (5%-phenyl)- methylpolysiloxane). A second GC column of 1 m × 0.25 mm ${}^1d_c$ × 0.25 μm ${}^2d_f$, DB-17 ms ((50%-phenyl)- methylpolysiloxane) was placed inside the secondary GC oven after the thermal modulator. Both columns were obtained from Agilent Technologies (Agilent Technologies J&W, Santa Clara, CA). The helium carrier gas (99.999% purity) flow rate was set to 2.0 mL/min at a corrected constant flow via pressure ramps. The inlet temperature was set at 280 °C. The primary column temperature was programmed with an initial temperature of 60 °C for 0.5 min and then increased at 5 °C/min to 280 °C and kept for 15 min. The secondary column temperature program was set to an initial temperature of 70 °C for 0.5 min and then also increased using the same temperature gradient employed in the first column to 280 °C. The thermal modulator was set to +15 °C relative to the secondary oven, and a modulation time of P_M = 2 s was used. The mass range was set as 29–800 *m/z* with an acquisition rate of 200 mass spectra per second. The ion source chamber was set at 230 °C with the transfer line temperature set to 280 °C, and the detector voltage was 1450 V with electron energy of 70 eV. The acceleration voltage was turned on after a solvent delay of 675 s. The split ratio was set at 20:1.

2.6. Data Analysis

The GC × GC-TOF MS data were processed using LECO's software ChromaTOF (version 4.50.8.0) for peak picking and tentative metabolite identification, followed by peak merging, peak list alignment, retention index filtering, normalization, and statistical significance test using MetPP.[21] Two-way ANOVA test with up to 1000-times sample permutation was used to determine whether a metabolite has a significance difference of abundance level between sample groups, where the threshold of probability was set $p < 0.05$.

Metabolite identification was achieved in three sequential steps. Mass spectrum matching was first employed to identify the top five matched candidate compounds for each experimental mass spectrum if the experimental mass spectrum and the best matched mass spectrum recorded in the NIST/ EPA/NIH Mass Spectral Library 2011 (NIST11) have a spectral similarity score higher than 600 regardless of the magnitude of the matching scores of the other top four ranked candidates. The tentatively assigned metabolites were then filtered by retention index matching using iMatch software with a p-value threshold of $p < 0.001$.[22] The best retention index matched metabolite was preserved if multiple tentatively assigned metabolites had the correct retention index values. To verify the identification of metabolites detected with significant abundance difference between sample groups, the authentic standards of these metabolites, if commercially available, were analyzed by GC × GC-TOF MS under the same experimental conditions as the biological samples analyzed. A tentative metabolite assignment was considered as a correct identification only if the experimental information on the authentic metabolite agreed with the corresponding information on the chromatographic peak in the biological samples, that is, difference of the first dimension retention time $\Delta^1 t_R \leq 10$ s, difference of the second dimension retention time $\Delta^2 t_R \leq 0.05$ s, and the mass spectral similarity $\Delta S \geq 700$.[20,23]

3. RESULTS

Six biological sample groups were formed in this study: rats fed with marginal copper without exposure to fructose (M-N, $n = 5$); rats fed with marginal copper and exposed to fructose (M-F, $n = 7$); rats fed with adequate copper without exposure to fructose (A-N, $n = 6$); rats fed with adequate copper and exposed to fructose (A-F, $n = 8$); rats fed with supplemental copper without exposure to fructose (S-N, $n = 7$); and rats fed with supplemental copper and exposed to fructose (S-F, $n = 8$).

Figure 1 depicts the histological analysis and hepatic triglyceride assay of rat liver tissue. Feeding rats with different levels of copper (i.e., marginal, adequate, or supplemental dose) without fructose for 4 weeks did not lead to obvious changes in liver histology (upper panel of Figure 1A). However, 4 weeks of feeding with high fructose led to obvious hepatic steatosis in both marginal copper deficient rats and copper supplementation rats compared to the controls, that is, sample group A-N (lower panel of Figure 1A). These changes were consistent with the hepatic triglyceride assay (Figure 1B).

Using GC × GC-TOF MS-based metabolomics, we examined whether different dietary doses of copper play a role in fructose-induced fatty liver by, respectively, studying the effects of copper, fructose, and their interaction on the fecal metabolite profiles of the six

sample groups. Figure 2 depicts clustering result of the metabolite profiles of the six sample groups using partial least-squares discriminant analysis (PLSDA). Figure S1 shows the results of cross-validation of the PLSDA model. High values of $Q^2 = 0.77$ and $R^2 = 0.94$ demonstrate very good predictive ability of the PLSDA model in clustering the rat fecal metabolites. Clear separation between the sample groups indicates that the significant difference in the rat fecal metabolome was caused by feeding rats with different doses of copper, with and without high fructose exposure.

Two-way ANOVA tests were employed to recognize metabolites with significant abundance changes between sample groups. Fold-change was defined as the ratio of the abundance value (peak area) of a metabolite in a test group divided by the abundance value of the same metabolite in a reference group. A total of 38 metabolites were detected with significant abundance level changes due to different doses of copper, fructose, or their synergetic interaction (Table 1). Among these metabolites, nine are amino acids, nine are fatty acids, and the other 20 metabolites include nonproteinogenic amino acids, organic acids, etc. The abundance level alteration of 24 metabolites (four fatty acids, four amino acids, 16 others) was induced by the copper concentration alone (i.e., p-1 ≤ 0.05). When the rats were exposed to a marginal level of copper, the mean fold-change of the nine fatty acids is 0.95 with standard error of the mean (SEM) 0.05, minimum 0.71, and maximum 1.21 (column M-N/A-N). When the rats were exposed to a supplemental level of copper, the mean fold-change of the nine fatty acids is 1.19 with SEM 0.25, minimum 0.59, and maximum 3.08 (column S-N/A-N). This may indicate that some of the fatty acid composition in rat fecal metabolome was more affected when the rats were exposed to the supplemental level of copper such as elaidic acid, pentadecylic acid, and paullinic acid (Table 1).

The high fructose affected the abundance level of 23 metabolites (i.e., p-2 ≤ 0.05), as listed in Table 1. A pronounced effect was observed in short chain fatty acids (SCFAs). Figure 3 shows four sample abundance distributions of four SCFAs, isobutyric acid, butyric acid, isovaleric acid, and valeric acid, in the six sample groups. The difference of the metabolite abundance levels among sample groups indicates that all four SCFAs were markedly decreased by excessive dietary fructose intake. However, this effect was independent of copper levels (ranging from 1.6–20 ppm). A similar effect was also observed in L-methionine and L-isoleucine (Table 1). While some SCFAs were decreased, some of the long chain fatty acids (LCFAs) were increased by high fructose feeding such as margaric acid and elaidic acid (Table 1).

A total of 12 metabolites have significant abundance level alterations between sample groups due to the synergistic interaction of copper and fructose (Table 1). The profound changes were observed in urea, glyceraldehyde, glycerol, D-pyroglutamic acid, and L-pyroglutamic acid. Among them, the greatest synergistic effects were observed between high fructose and high copper level, whereas some effects were due to high fructose and marginal copper.

To understand the inter-relationships between the metabolites with significant abundance changes between sample groups, all 38 metabolites listed in Table 1 were submitted to Ingenuity Pathway Analysis (IPA) to correlate these metabolites with potential metabolic

pathways. Of the 38 metabolites, 31 were mapped into the IPA database. These mapped metabolites are mainly related to inflammatory diseases and responses. Sixteen metabolites were mapped to the most probable metabolite associated network functions entitled Increased Levels of Albumin, Amino Acid Metabolism, Small Molecule Biochemistry, with a score of 37 (Figure S2A). The second most probable network function is Connective Tissue, Development and Function, Tissue Morphology, Carbohydrate Metabolism that contains nine matched metabolites with a score of 21 (Figure S2B). IPA also recognized that the top hepatotoxicity is liver steatosis and inflammation/hepatitis.

4. DISCUSSION

The importance of gut microbiota in the development of obesity and the metabolic syndrome is increasingly being recognized. However, the underlying mechanisms remain largely unknown. The composition of the gut microbial community is closely related to the diet consumed and is highly modifiable.[24] One of the functional roles of gut microbiota is the generation of metabolites by breaking down the protein, amino acids, and nondigestible carbohydrates of the diet, which contribute to energy and protein homeostasis between host and microbial community.[25] In this study, we aimed to define the effects of two crucial dietary factors, fructose and copper, that are highly relevant to the development of NAFLD on the alteration of gut metabolites.

Among the identified 38 fecal metabolites with significant abundance level changes induced by different dietary doses of copper or high fructose (Table 1), one of the most prominent findings is the significantly decreased SCFAs that were solely caused by high fructose feeding, independent of dietary copper (ranging from marginal (1.6 ppm) to supplemental (20 ppm) dose). SCFAs are the principal metabolites generated from the dietary carbohydrate fermentation by colon bacteria normally occurring in the ascending colon. We detected four SCFAs, including valeric acid, butyric acid, isovaleric acid, and isobutyric acid, as having major abundance changes. Among them, butyric acid is the major energy source for colonocytes, and it plays important roles in maintaining gut barrier function and modulating microbiota components.[26] Despite the increased carbohydrate substrate from fructose (branched chain fatty acids: isobutyric acid and isovaleric acid are from amino acids),[27] the four SCFAs are all decreased. This suggests that the decrease in SCFAs is not a direct effect of fructose and may possibly be due to decreased butyrate generating bacteria that are associated with the excessive fructose intake. Another important finding is the marked increased elaidic acid by high fructose feeding. The abundance level of elaidic acid increased more than three-fold in the rats fed with copper supplementation diet irrespective of fructose consumption, suggesting that both dietary inappropriate copper and fructose intake have a profound effect on the elaidic acid generation. Elaidic acid is a major source of industrially produced trans-fatty acid in food stuffs, and transfats are well-known to be deleterious to human health. Of note, even consumed in low amounts, elaidic acid increases visceral fat and liver fat accumulation in rats.[28] In addition, two LCFAs, margaric acid (C17:0) and pentadecylic acid (C15:0), are impacted by dietary copper and fructose consumption. Margaric acid was increased mainly by excessive fructose intake, and pentadecylic acid was increased by highdose copper. Most strikingly, both of these LCFAs can only be produced by bacteria, suggesting that dietary copper and fructose may modify

the gut microbiota phylum profile, which might favor the growth of C15:0 and C17:0 generating bacteria. However, whether and how these bacteria species contribute to the metabolic phenotype remain to be determined.

Dietary proteins not assimilated in the upper gastrointestinal tract may enter the colon, wherein they are hydrolyzed to amino acids, which are then available for utilization by bacteria.[29] The gut microbiota plays a critical role in amino acid hemostasis. Amino acids not only support the growth of bacteria, but also can be synthesized by the bacteria.[30] The pronounced alterations of fecal amino acids we found include: decreased L-methionine and L-isoleucine; and increased L-threonine, L-aspartic acid, and L-glutamic acid. Decreased L-methionine and L-isoleucine are likely associated with the dietary high fructose intake. Methionine is an essential amino acid, which plays important roles in the transsulfuration pathway and phospholipid synthesis. Methionine deficiency is a contributing factor to the development of hepatic steatohepatitis.[31] However, whether decreased fecal methionine can predict the systemic methionine levels remains to be determined. In addition, decreased L-isoleucine parallels the decreased isovaleric acid, indicating that decreased isovaleric acid might be attributed to decreased precursor, L-isoleucine.[32] L-Threonine was significantly increased by both marginal copper and copper supplementation diet, and it was further increased by high fructose feeding in copper supplementation diet fed rats, whereas high fructose intake led to decreased L-threonine in marginal copper deficient rats. L-threonine is also an essential amino acid. Both methionine and threonine can be synthesized by microorganisms from aspartic acid. However, the reasons for the discrepancy between the alterations of these two amino acids are unclear, possibly related to the changed microbiota. Both L-aspartic acid and L-glutamic acid were markedly increased by high fructose feeding and further increased by marginal copper or copper supplementation diet, with more pronounced effect on L-aspartic acid. The luminal amino acids could be either the substrates or products of gut bacteria. Their functional roles are unclear. However, combining these luminal profiles with serum amino acids profiles will help to better understand their biological functions.

Urea is generated in the liver and passed into the gut, in which it is hydrolyzed to ammonia by the gut microbiota.[33] In the current study, we found that fecal urea was increased by fructose feeding in adequate copper fed animals, whereas robustly increased urea (>4-fold) was observed in the marginal copper deficient rats, irrespective of fructose intake. In addition, a synergistic effect on fecal urea production was seen in copper supplementation and high fructose fed rats, with up to a six-fold increase. It seems that accumulated urea in the feces is likely due to the impaired breakdown by the gut bacteria.

Malic acid is an intermediate of the tricarboxylic acid cycle that is an energy metabolite.[34] It was significantly increased by both dietary high fructose intake and marginal copper or copper supplementation diet. Moreover, the more profound effect was seen in the copper supplementation diet and high fructose fed rats, which parallels the amount of fat accumulation in the liver. However, it remains to be determined whether increased fecal malic acid contributes to increased energy harvesting.

5-Aminovaleric acid (5-AV) is a metabolite of protein degradation by several anaerobic bacteria that cannot be detected in germ-free mice.[35] We found that 5-AV was significantly reduced by either marginal copper or copper supplementation diet. It was also markedly increased with fructose feeding, particularly in marginal copper deficient rats. This suggests that the 5-AV generating bacteria were enhanced by the combination of marginal copper and high fructose feeding.

In particular, the significant altered abundance in some of the metabolites was attributed to the synergistic effect of fructose and copper level such as glyceraldehyde, an intermediate of glycolysis, and *de novo* lipogenesis. The elevated fecal glyceraldehyde induced by fructose–copper interaction paralleled the amount of hepatic fat accumulation, suggesting it may contribute to the pathogenesis of fatty liver. We also observed the significant increased pyroglutamic acid by the fructose– copper interaction, suggesting the disturbance of glutathione metabolism[36] likely due to the altered gut microbiota. However, how those metabolites regulate hepatic lipid metabolism remains to be further determined.

In summary, our data revealed a distinct fecal metabolomics profile associated with the dietary high fructose and different doses of copper intake. The unique fecal metabolomics signature associated with the specific dietary components enables the identification of potential biomarkers. However, the addition of a metagenomics study will help to better understand the contribution(s) of gut microbiota to the alterations of fecal metabolomics. Moreover, the biological functions of the altered fecal metabolites require more mechanistic study. Simultaneous plasma and liver metabolomics analysis will provide a more comprehensive and integrative metabolites profile.

It should also be noted that we extracted metabolites from rat feces using a solvent mixture of methanol and water. The hydrophobic metabolites such as triglycerides were not analyzed, and their regulation information was lost in this study. The extracted metabolites were derivatized using MTBSTFA and analyzed on GC × GC-TOF MS. Compared with conventional GC-MS, GC × GC-TOF MS has a much increased separation power.[37] However, the metabolites presented in the extracted fecal samples may still be well beyond the separation power of the GC × GC-TOF MS system. For this reason, some low abundance metabolites may not have been detected. Furthermore, the derivatized metabolites were identified by matching the experimental mass spectra to the mass spectra recorded in the NIST11 library. The NIST11 main library contains 243 893 election ionization (EI) mass spectra for 212 961 compounds, of which fewer than 2000 MTBSTFA derivatized compounds have their EI mass spectra. Therefore, it is possible that an MTBSTFA derivatized metabolite that does not have EI mass spectra in the NIST11 library can be identified as another compound. For this reason, we removed all metabolites that were identified by ChromaTOF as derivatized metabolites by other derivatization reagents. Third, the GC × GC-TOF MS instrument was set to collect data after the solvent chromatographic peak. Some metabolites such as the SCFAs, formic acid, ethanoic acid, and propanoic acid, have low boiling points. These metabolites eluted earlier than the solvent and were not detected in this study. Lastly, GC × GC-TOF MS can only detect the metabolites that are volatile or volatile after derivatization. Some metabolites in the extracted fecal samples thus

may not be detected. Analyzing the metabolite extracts on both the liquid chromatography (LC)–MS and GC × GC-TOF MS platforms is an option of increasing metabolite coverage.

5. CONCLUSIONS

GC × GC-TOF MS analysis of rat fecal samples revealed distinct fecal metabolome profiles associated with the dietary high fructose and different doses of copper intake, the two risk factors involved in the etiology of NAFLD. Among the 38 metabolites identified with significant abundance change between sample groups, some of them are clearly related to the alteration of gut microbiota associated with dietary copper or fructose intake, including SCFAs, C15:0 and C17:0, LCFAs, urea, 5-AV, and two essential amino acids (L-methionine and L-isoleucine). Robustly increased malic acid correlates with the excessive fructose intake and was further enhanced by copper intake. Our results indicate that fecal metabolite analysis provides novel insights into the role of gut microbiota in the development of NAFLD and open new avenues for future research.

Supplementary Material

Refer to Web version on PubMed Central for supplementary material.

ACKNOWLEDGMENTS

The authors thank Mrs. Marion McClain for review of this manuscript. This work was supported by National Institute of Health (NIH) Grant Nos. P30AA019360, R01DK055030 and RO1DK071765; National Science Foundation Grant No. DMS-1312603; the Veterans Administration; and the UofL Clinical and Translational Pilot Program.

REFERENCES

(1). Williams CD; Stengel J; Asike MI; Torres DM; Shaw J; Contreras M; Landt CL; Harrison SA Prevalence of nonalcoholic fatty liver disease and nonalcoholic steatohepatitis among a largely middle-aged population utilizing ultrasound and liver biopsy: a prospective study. Gastroenterology 2011, 140, 124–31. [PubMed: 20858492]

(2). Tilg H; Moschen AR Evolution of inflammation in nonalcoholic fatty liver disease: the multiple parallel hits hypothesis. Hepatology 2010, 52, 1836–46. [PubMed: 21038418]

(3). Tolman KG; Fonseca V; Dalpiaz A; Tan MH Spectrum of liver disease in type 2 diabetes and management of patients with diabetes and liver disease. Diabetes Care 2007, 30, 734–43. [PubMed: 17327353]

(4). de Alwis NM; Day CP Non-alcoholic fatty liver disease: the mist gradually clears. J. Hepatol 2008, 48, S104–12. [PubMed: 18304679]

(5). Bray GA Potential health risks from beverages containing fructose found in sugar or high-fructose corn syrup. Diabetes Care 2013, 36, 11–2. [PubMed: 23264287]

(6). Dhingra R; Sullivan L; Jacques PF; Wang TJ; Fox CS; Meigs JB; D'Agostino RB; Gaziano JM; Vasan RS Soft drink consumption and risk of developing cardiometabolic risk factors and the metabolic syndrome in middle-aged adults in the community. Circulation 2007, 116, 480–8. [PubMed: 17646581]

(7). Ouyang X; Cirillo P; Sautin Y; McCall S; Bruchette JL; Diehl AM; Johnson RJ; Abdelmalek MF Fructose consumption as a risk factor for non-alcoholic fatty liver disease. J. Hepatol 2008, 48, 993–9. [PubMed: 18395287]

(8). Jin R; Le NA; Liu S; Farkas Epperson M; Ziegler TR; Welsh JA; Jones DP; McClain CJ; Vos MB Children with NAFLD are more sensitive to the adverse metabolic effects of fructose beverages

than children without NAFLD. J. Clin. Endocrinol. Metab 2012, 97, E1088–98. [PubMed: 22544914]

(9). Le KA; Ith M; Kreis R; Faeh D; Bortolotti M; Tran C; Boesch C; Tappy L Fructose overconsumption causes dyslipidemia and ectopic lipid deposition in healthy subjects with and without a family history of type 2 diabetes. Am. J. Clin. Nutr 2009, 89, 1760–5. [PubMed: 19403641]

(10). Stanhope KL; Schwarz JM; Keim NL; Griffen SC; Bremer AA; Graham JL; Hatcher B; Cox CL; Dyachenko A; Zhang W; McGahan JP; Seibert A; Krauss RM; Chiu S; Schaefer EJ; Ai M; Otokozawa S; Nakajima K; Nakano T; Beysen C; Hellerstein MK; Berglund L; Havel PJ Consuming fructose-sweetened, not glucose-sweetened, beverages increases visceral adiposity and lipids and decreases insulin sensitivity in overweight/obese humans. J. Clin. Invest 2009, 119, 1322–34. [PubMed: 19381015]

(11). Tappy L; Le KA Metabolic effects of fructose and the worldwide increase in obesity. Physiol. Rev 2010, 90, 23–46. [PubMed: 20086073]

(12). Bergheim I; Weber S; Vos M; Kramer S; Volynets V; Kaserouni S; McClain CJ; Bischoff SC Antibiotics protect against fructose-induced hepatic lipid accumulation in mice: role of endotoxin. J. Hepatol 2008, 48, 983–92. [PubMed: 18395289]

(13). Spruss A; Kanuri G; Wagnerberger S; Haub S; Bischoff SC; Bergheim I Toll-like receptor 4 is involved in the development of fructose-induced hepatic steatosis in mice. Hepatology 2009, 50, 1094104.

(14). Fields M; Ferretti RJ; Smith JC Jr.; Reiser S The interaction of type of dietary carbohydrates with copper deficiency. Am. J. Clin. Nutr 1984, 39, 289–95. [PubMed: 6695829]

(15). Song M; Schuschke DA; Zhou Z; Chen T; Pierce WM Jr.; Wang R; Johnson WT; McClain CJ High fructose feeding induces copper deficiency in Sprague-Dawley rats: a novel mechanism for obesity related fatty liver. J. Hepatol 2012, 56, 433–40. [PubMed: 21781943]

(16). Song M; Schuschke DA; Zhou Z; Chen T; Shi X; Zhang J; Zhang X; Pierce WM Jr.; Johnson WT; Vos MB; McClain CJ Modest fructose beverage intake causes liver injury and fat accumulation in marginal copper deficient rats. Obesity 2013, 21, 1669–75. [PubMed: 23512597]

(17). Aigner E; Strasser M; Haufe H; Sonnweber T; Hohla F; Stadlmayr A; Solioz M; Tilg H; Patsch W; Weiss G; Stickel F; Datz C A role for low hepatic copper concentrations in nonalcoholic Fatty liver disease. Am. J. Gastroenterol 2010, 105, 1978–85. [PubMed: 20407430]

(18). Aigner E; Theurl I; Haufe H; Seifert M; Hohla F; Scharinger L; Stickel F; Mourlane F; Weiss G; Datz C Copper availability contributes to iron perturbations in human nonalcoholic fatty liver disease. Gastroenterology 2008, 135, 680–8. [PubMed: 18505688]

(19). Bligh EG; Dyer WJ A rapid method of total lipid extraction and purification. Can. J. Biochem. Physiol 1959, 37, 911–7. [PubMed: 13671378]

(20). Shi X; Wei X; Yin X; Wang Y; Zhang M; Zhao C; Zhao H; McClain CJ; Feng W; Zhang X Hepatic and fecal metabolomic analysis of the effects of Lactobacillus rhamnosus GG on alcoholic fatty liver disease in mice. J. Proteome Res 2015, 14, 1174–1182. [PubMed: 25592873]

(21). Wei X; Shi X; Koo I; Kim S; Schmidt RH; Arteel GE; Watson WH; McClain C; Zhang X MetPP: a computational platform for comprehensive two-dimensional gas chromatography time-of-flight mass spectrometry-based metabolomics. Bioinformatics 2013, 29, 1786–92. [PubMed: 23665844]

(22). Zhang J; Fang AQ; Wang B; Kim SH; Bogdanov B; Zhou ZX; McClain C; Zhang X iMatch: A retention index tool for analysis of gas chromatography-mass spectrometry data. Journal of Chromatography A 2011, 1218, 6522–6530. [PubMed: 21813131]

(23). Shi X; Wei X; Koo I; Schmidt RH; Yin X; Vaughn A; Kim SH; McClain CJ; Arteel GE; Zhang X; Watson WH Metabolomic analysis of the effects of chronic arsenic exposure in a mouse model of diet-induced fatty liver disease. J. Proteome Res 2014, 13, 547–554. [PubMed: 24328084]

(24). Konrad D; Wueest S The Gut-Adipose-Liver Axis in the Metabolic Syndrome. Physiology 2014, 29, 304–313. [PubMed: 25180260]

(25). Louis P; Hold GL; Flint HJ The gut microbiota, bacterial metabolites and colorectal cancer. Nat. Rev. Microbiol 2014, 12, 66172.

(26). Ploger S; Stumpff F; Penner GB; Schulzke JD; Gabel G; Martens H; Shen Z; Gunzel D; Aschenbach JR Microbial butyrate and its role for barrier function in the gastrointestinal tract. Ann. N. Y. Acad. Sci 2012, 1258, 52–9. [PubMed: 22731715]

(27). Blachier F; Mariotti F; Huneau JF; Tome D Effects of amino acid-derived luminal metabolites on the colonic epithelium and physiopathological consequences. Amino Acids 2007, 33, 547–62. [PubMed: 17146590]

(28). Dorfman SE; Laurent D; Gounarides JS; Li X; Mullarkey TL; Rocheford EC; Sari-Sarraf F; Hirsch EA; Hughes TE; Commerford SR Metabolic implications of dietary trans-fatty acids. Obesity 2009, 17, 1200–7. [PubMed: 19584878]

(29). Nyangale EP; Mottram DS; Gibson GR Gut microbial activity, implications for health and disease: the potential role of metabolite analysis. J. Proteome Res 2012, 11, 5573–85. [PubMed: 23116228]

(30). Yang YX; Dai ZL; Zhu WY Important impacts of intestinal bacteria on utilization of dietary amino acids in pigs. Amino Acids 2014, 46, 2489–501. [PubMed: 25063203]

(31). Pickens MK; Yan JS; Ng RK; Ogata H; Grenert JP; Beysen C; Turner SM; Maher JJ Dietary sucrose is essential to the development of liver injury in the methionine-choline-deficient model of steatohepatitis. J. Lipid Res 2009, 50, 2072–82. [PubMed: 19295183]

(32). Cummings JH; Englyst HN Fermentation in the human large intestine and the available substrates. Am. J. Clin. Nutr 1987, 45, 1243–55. [PubMed: 3034048]

(33). Hooper LV; Midtvedt T; Gordon JI How host-microbial interactions shape the nutrient environment of the mammalian intestine. Annu. Rev. Nutr 2002, 22, 283–307. [PubMed: 12055347]

(34). Velagapudi VR; Hezaveh R; Reigstad CS; Gopalacharyulu P; Yetukuri L; Islam S; Felin J; Perkins R; Boren J; Oresic M; Backhed F The gut microbiota modulates host energy and lipid metabolism in mice. J. Lipid Res 2010, 51, 1101–12. [PubMed: 20040631]

(35). Claus SP; Tsang TM; Wang Y; Cloarec O; Skordi E; Martin FP; Rezzi S; Ross A; Kochhar S; Holmes E; Nicholson JK Systemic multicompartmental effects of the gut microbiome on mouse metabolic phenotypes. Mol. Syst. Biol. 2008, 4, 219. [PubMed: 18854818]

(36). Lord RS; Bralley JA Clinical applications of urinary organic acids. Part I: Detoxification markers. Alt. Med. Rev 2008, 13, 205–15.

(37). Winnike J; Wei ×; Knagge K; Colman S; Gregory S; Zhang × Comparison of GC-MS and GC × GC-MS in the Analysis of Human Serum Samples for Biomarker Discovery. J. Proteome Res 2015, 14, 1810–7. [PubMed: 25735966]

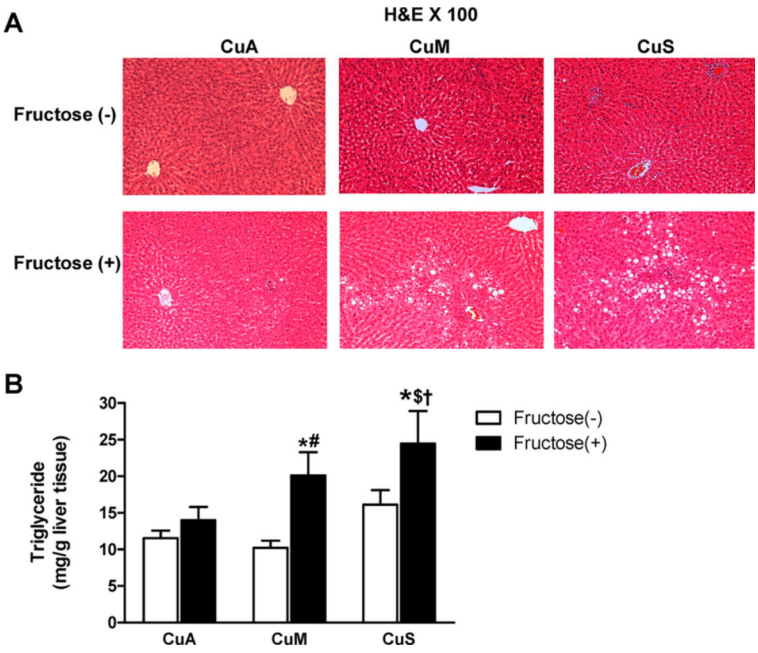

Figure 1.

Effect of dietary different doses of copper and high fructose feeding on liver fat accumulation. (A) Representative photomicrographs of the H&E staining of liver section (100×). The red background is cell cytoplasm, black dots are cell nucleii, and the white color is fat droplets. (B) Hepatic triglycerides. Data represent means ± SD (n = 5–8). *, versus CuA without fructose; #, versus CuM without fructose; $, versus CuS without fructose; †, versus CuA with fructose ($p \leq 0.05$, two-way ANOVA). CuA, adequate copper diet; CuM, marginal copper deficient diet; CuS, copper supplementation diet.

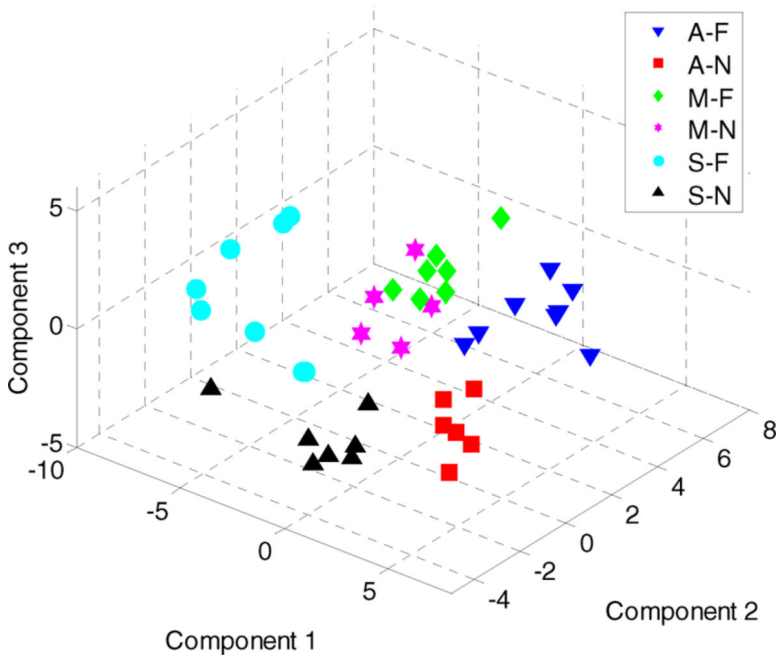

Figure 2.
Clustering of metabolite profiles using PLSDA.

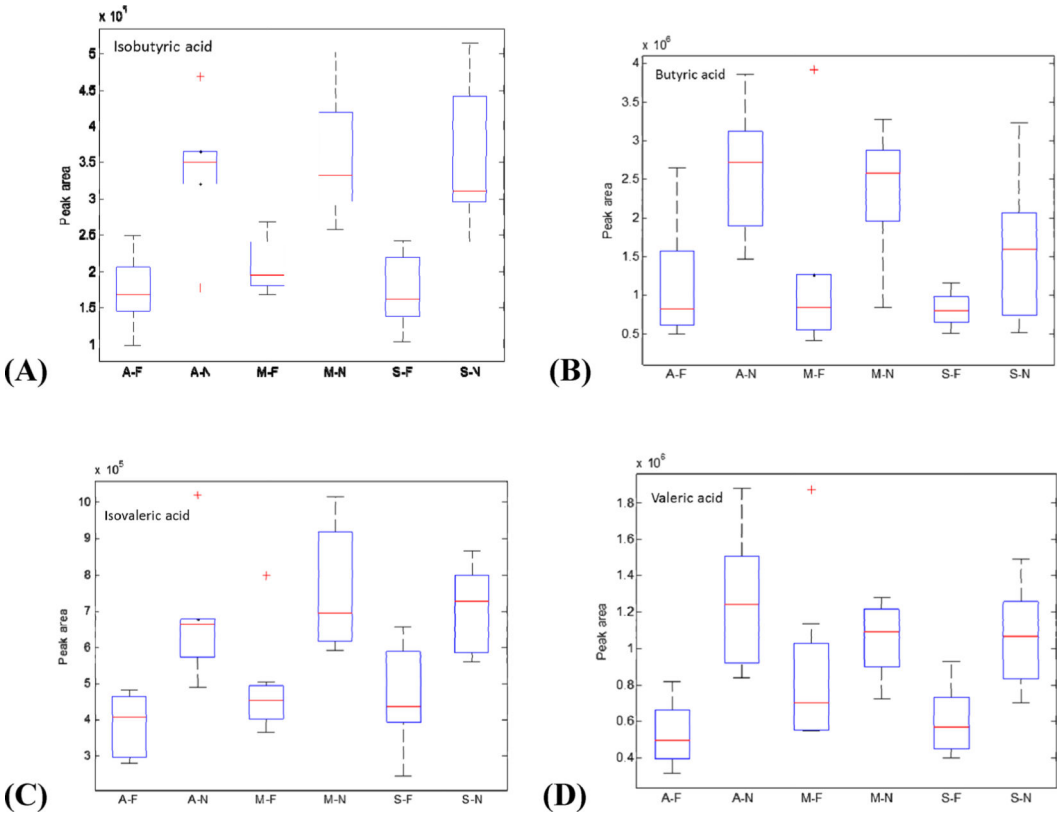

Figure 3.

Abundance distribution of metabolite (A) isobutyric acid, (B) butyric acid, (C) isovaleric acid, and (D) valeric acid in six sample groups.

Table 1.

Metabolites with Significant Changes of Abundance Level among the Six Sample Groups

name	CAS	^1t_R (s)	^2t_R (s)	fold change									
				M-N/A-N[a]	S-N/A-N[b]	A-F/A-N[c]	M-F/A-N[d]	S–F/A-N[e]	M-F/M-N[f]	S-F/S-N[g]	*p*-1[h]	*p*-2[i]	*p*-3[j]
Fatty Acids													
valeric acid	109–52–4	964	1.22	0.83	0.84	0.42	0.48	0.48	0.58	0.56		0	
butyric acid	107–92–6	804	1.19	0.89	0.59	0.44	0.32	0.31	0.36	0.52		1.02×10^{-5}	
margaric acid	506–12–7	2486	1.32	1.21	0.86	1.41	1.46	1.24	1.21	1.44		2.1×10^{-3}	
elaidic acid[k]	112–79–8	2610	1.45	0.71	3.08	1.94	1.99	3.38	2.81	1.10	5.9×10^{-5}	3.6×10^{-2}	
stearic acid	57–11–4	2626	1.44	0.90	0.60	1.11	1.01	0.48	1.12	0.81	2.6×10^{-5}		
pentadecylic acid	1002–84–2	2286	1.31	0.92	1.31	0.78	0.92	1.84	0.99	1.40	4.7×10^{-4}		
paullinic acid[k]	17735–94–3	2854	1.82	0.92	1.29	1.03	0.82	2.12	0.89	1.64	4.9×10^{-4}		
isovaleric acid[k]	503–74–2	886	1.19	1.12	1.03	0.63	0.63	0.68	0.57	0.67		0	
isobutyric acid[k]	79–31–2	728	1.14	1.06	1.07	0.51	0.62	0.51	0.58	0.48		0	
Amino Acids													
L-methionine	63–68–3	2058	1.38	0.92	0.73	0.71	0.80	0.71	0.87	0.97		1.2×10^{-2}	
L-lysine	56–87–1	2504	1.28	1.03	0.79	0.83	0.93	1.16	0.90	1.47			3.0×10^{-4}
L-threonine	72–19–5	2116	1.22	3.03	1.93	1.91	1.16	3.00	0.38	1.55	1.2×10^{-4}		0
L-leucine	61–90–5	1718	1.21	0.92	1.02	0.79	0.95	0.93	1.02	0.90		3.6×10^{-2}	
L-aspartic acid	56–84–8	2266	1.30	1.85	1.83	2.04	2.32	2.84	1.26	1.55	7.2×10^{-3}	1.5×10^{-3}	
L-proline	147–85–3	1814	1.33	1.16	1.35	0.86	1.19	1.38	1.03	1.02	6.3×10^{-3}		
L-glutamic acid[k]	56–86–0	2394	1.31	1.26	1.21	1.23	1.38	1.73	1.09	1.43	3.1×10^{-4}	2.0×10^{-4}	
L-isoleucine	73–32–5	1760	1.22	0.90	0.96	0.68	0.89	0.83	0.99	0.87			
L-serine	56–45–1	2080	1.22	0.95	0.82	0.83	0.97	1.04	1.02	1.27			2.1×10^{-3}
Others													
methoxyacetic acid[k]	625–45–6	1402	1.18	2.63	1.91	1.72	1.64	3.04	0.62	1.59	0	6.3×10^{-3}	0
3-methylpentanoic acid[k]	105–43–1	1124	1.23	1.94	1.87	0.81	1.22	1.48	0.63	0.79	0	3.9×10^{-5}	
urea	57–13-6	1662	1.42	4.87	1.12	1.40	4.12	5.96	0.84	5.34	3.1×10^{-5}	2.5×10^{-3}	1.3×10^{-4}

name	CAS	$^{1}t_R$ (s)	$^{2}t_R$ (s)	fold change									
				M-N/A-N[a]	S-N/A-N[b]	A-F/A-N[c]	M-F/A-N[d]	S–F/A-N[e]	M-F/M-N[f]	S-F/S-N[g]	*p*-1[h]	*p*-2[i]	*p*-3[j]
glyceraldehyde[k]	56–82–6	1672	1.28	2.21	1.50	1.66	2.31	2.95	1.04	1.97	3.0×10^{-4}	1.1×10^{-3}	2.7×10^{-2}
nonanedioic acid[k]	123–99–9	2402	1.39	2.60	1.32	1.04	1.88	0.62	0.72	0.47	5.1×10^{-4}	2.8×10^{-2}	
hypoxanthin[k]	68–94–0	2354	1.75	1.24	1.17	1.08	1.17	1.37	0.94	1.18	2.9×10^{-2}		
ethyene glycol[k]	107–21–1	1310	1.15	1.44	1.20	1.34	1.29	1.58	0.90	1.32	3.6×10^{-2}	2.2×10^{-2}	1.3×10^{-2}
glycerol[k]	56–81–5	1948	1.15	1.29	1.40	1.34	1.05	1.39	0.81	1.00	1.6×10^{-3}		4.7×10^{-4}
D-pyroglutamic acid	4042–36–8	2386	1.16	1.55	1.60	1.32	1.61	3.08	1.04	1.97	4.3×10^{-5}	1.8×10^{-3}	2.1×10^{-2}
nicotinic acid[k]	59–67–6	1508	1.56	1.31	1.29	1.10	1.19	1.67	0.91	1.29	6.9×10^{-4}		
4-imidazoleacrylic acid[k]	104–98–3	2628	1.94	1.26	1.30	1.02	1.54	1.54	0.98	1.18	2.2×10^{-2}		
malic acid	6915–15–7	2219	1.28	3.84	3.18	5.65	5.14	8.45	1.34	2.66	3.5×10^{-3}	4.1×10^{-6}	
17-octadecynoic acid	34450–18–5	2594	1.48	0.46	0.76	0.77	0.99	0.98	2.15	1.30		3.7×10^{-2}	3.9×10^{-3}
phenylacetic acid	103–82–2	1488	1.53	1.04	0.95	0.59	0.60	0.86	0.57	0.90		2.0×10^{-6}	2.2×10^{-2}
α-aminobutyric acid	2835–81–6	1596	1.21	1.00	1.12	0.78	0.99	2.29	0.99	2.05	8.4×10^{-3}		
L-pyroglutamic acid	98–79–3	2038	1.50	1.33	0.99	1.08	1.20	1.53	0.90	1.54			2.6×10^{-2}
5-aminovaleric acid	660–88–8	1940	1.28	0.40	0.21	0.56	2.62	0.35	6.58	1.66	9.1×10^{-3}	1.0×10^{-2}	
4-aminobenzoic acid	150–13–0	1999	1.99	1.10	0.78	0.63	1.39	0.51	1.26	0.66	3.3×10^{-5}		1.7×10^{-2}
benzoic acid	65–85–0	1434	1.5	1.29	1.04	1.16	1.10	0.60	0.85	0.58	1.4×10^{-3}		5.0×10^{-3}
α-hydroxyglutaric acid	2889–31–8	2332	1.30	1.65	1.18	1.68	1.66	1.39	1.00	1.18		2.9×10^{-2}	

[a] Fold change for M-N to A-N.

[b] Fold change for S-N to A-N.

[c] Fold change for A-F to A-N.

[d] Fold change for M-F to A-N.

[e] Fold change for S-F to A-N.

[f] Fold change for M-F to M-N.

[g] Fold change for S-F to S-N.

[h] *P*-value of Cu.

[i] *P*-value of factor fructose.

[j] *P*-value of the interaction of Cu and fructose.

[k] Tentative identification without verification using authentic standards.